INDIAN JOURNAL OF SCIENCE AND TECHNOLOGY

ORIGINAL ARTICLE

Check for updates

OPEN ACCESS

Received: 04/12/2024

Accepted: 06/05/2025

Published: 10/06/2025

Citation: Nath V, Sambariya DK (2025) Application of Optimized PI-PD Controller for Load Frequency Control in Deregulated Environment. Indian Journal of Science and Technology 18(22): 1768-1781. https://doi.org/10.17485/IJST/v18i22.3938

* **Corresponding author**.

Viveknath311989@gmail.com

Funding: None

Competing Interests: None

Published By Indian Society for Education and Environment (iSee)

ISSN
Print: 0974-6846
Electronic: 0974-5645

Application of Optimized PI-PD Controller for Load Frequency Control in Deregulated Environment

Vivek Nath[1]*, D. K. Sambariya[1]

1 Rajasthan Technical University, Kota, Rajasthan, India

Abstract

Objectives: The deregulation of power networks has produced new obstacles for Load Frequency Control (LFC) due to the increased complexity caused by Generation Companies (GENCOS) functioning individually in a competitive world. The objective of this study is to expand LFC presentation in a deregulated environment by optimizing a Proportional-Integral-Proportional-Derivative (PI-PD) controller with the Artificial Bee Colony (ABC) optimized technique. A robust and adaptive control method is tried to develop for (GENCOS). **Method:** The Simulations are conducted using MATLAB 2018 version. The study adopts a full dynamic model of a deregulated multi-area multi-source interlinked power system (MAMS-IPS) having Thermal-Hydro-Gas generating units following AVR in both interconnected areas. Also taking into account the interactions between generation companies (GENCOS), Transmission Companies (TRANSCOS), and Distribution Companies (DISCOS), the study is further expanded by adding a magnetic storage device (SMES), followed by a FACTs Device (UPFC). Its effects are absorbed by frequency and Tie-line power variation. **Finding:** The ABC-based PI-PD controller method intends to reduce performance indices such as ISE, IAE, ITSE, and ITAE. Settling time and Peak overshoot of responses are reduced. The result of the suggested controller is compared with recently published novel techniques. Settling time for frequency and Tie-line power responses are 5.2456 sec, 8.6810 sec, and 11.58 sec which are quite better as compared to the result of novel techniques of literature. Peak time is also improved impressively it is 0.000231 sec and 0.00004019 sec for frequency deviation and 0.0001745 sec for tie-line power variation. Eigenvalues analysis is conducted to comment on the stability of the power system. **Novelty:** Nonlinearities such as GRC, GDB, and Boiler are introduced in MAMS-IPS. Simulation findings show that the suggested approach improves frequency regulation, reduces settling time (ST), and increases system stability. The robustness of the proposed controller under varied loading circumstances is investigated.

Keywords: Superconducting Magnetic Energy Storage (SMES); Unified Power Flow Control (UPFC); Governor Dead Band (GDB); Governor Rate Constraints (GRC); Proportional Integral-Proportional Derivative (PI-PD); Artificial Bee Colony (ABC)

1 Introduction

Load Frequency Control (LFC) is an important component of the electricity supply system functioning, providing a balance between electrical generation and consumption to preserve grid stability. In the current electricity environment, integrating different generating units from different parts of the world in a multi-source energy system raises serious problems for LFC. In this study paper, each location has three generating units, including thermal, hydro, and gas-based ones. The major goal of this project is to develop and implement an effective control strategy that is capable of maintaining the balance between generation and demand in an interconnected electrical system [(1)]. The intention is to increase the overall performance of the power system while taking into account challenges like inter-area power exchanges, transmission delays, and the intrinsic nonlinearity of individual generating units. MAMS-IPS introduces nonlinearity restrictions such as governor dead band (GDB), governor rate constraints (GRC), and boiler. The research is enlarged by including an Automatic Voltage Regulator (AVR) in each interrelated region as given in [(2)]. This capability guarantees not only load frequency management but also voltage stability, providing the total demands of a stable power network. In deregulated surroundings, knowing the roles of Generation Companies (GENCOs), Transmission Companies (TRANSCOs), and Distribution Companies (DISCOs) is critical. The interplay between these variables complicates load frequency management, posing a powerful and adaptive control mechanism. Initially, a single governing organization known as a vertically integrated utility (VIU) helped oversee power generation, transmission, and distribution while selling it at a set tariff. The reformed energy market created new autonomous entities, such as distributor businesses (DISCO), generator firms (GENCO), transmission trades (TRANSCO), and independent power producers (IPP). In a deregulated power system (PS), the self-governing system operator (ISO) controls frequency adjustments and power flow between the lines within specific restrictions. The DISCO Participation Matrix (DPM) for the Reorganize architecture was presented in [(3)] by analysing the power system's multilateral agreements. In this article three cases are considered for analysing the deregulated environment in detail. Literature survey: In this literature, an interlinked Power System (IPS) consists of several generating sources incorporated with SMES and UPFC is considered in a deregulated atmosphere is illustrated in [(4)]. Optimized technique known as an ICA used for tuning Fuzzy PID-filter (1 + PI) regulator, known as FPIDF (1 + PI), is implemented as a supplementary supervisor for LFC following with CES-RFB is given in [(5)]. Aquila optimization technique is illustrated for tuning the parameter of fractional order PID controller demonstrated for LFC in deregulated scenario [(6)]. Hybrid TLBO and pattern search techniques are suggested for automatically controlling power generation applied in a restricted environment given in [(7)]. A Slap swarm approach (SSA) improved fuzzy-based proportional-integral-derivative filter (FPIDF) regulator with a redox flow battery (RFB) to decrease frequency deviation is provided in [(8)]. An FOI-PD Controller whose parameters tuned by Fitness Dependent Optimizer based improvised technique for Automatic Control in Deregulated Environments is illustrated in [(1)].

Furthermore, SMES and UPFC are incorporated for improving effectively, the overall functionality of the electrical system. A UPFC-SMES-based 3DOF-PID Regulator for LFC of a green energy source-based Electrical Network under Regulation Employing GOA is shown in [(9)]. Role of SMES devices in regulating power system for stabilizing the frequencies in a deregulated environment is illustrated in [(10)]. Different soft computing application for LFC is illustrated in [(11)] showing the advantages of TID, PI-PD, PD-PID for improving the steady-state error of output responses of the Plant. A Fuzzy-PID based controller whose parameters are optimized using the whale optimization algorithm (WOA) is executed for dynamics control of a MAMS-IPS for Deregulated Power network is provided in [(12)]. The usefulness of the suggested control technique is assessed using comprehensive performance indicators. The objective functions are the Integral of Time-weighted Absolute Error (ITAE), Integral of Squared Error (ISE), Integral of Time multiplied Squared Error (ITSE), and Integral of Absolute Error.

Research Gap:

In this article, MAMS-IPS unified with three generating units is considered for LFC investigation, and the result of energy storage device (SMES) and FACT device is not included. Additionally, MAMS-IPS does not evaluate the influence of nonlinearity and Automatic Voltage Regulation (AVR) [(13)]. This study has considered optimized fractional controller for restricted environment power system incorporated with UPFC [(14)]. But AVR and SMES along with nonlinearities are not considered. This article considers the impact of nonlinearities like as GRC and GDB, as well as AVR and UPFC devices with AC-link subsequent energy storage devices. The effect of voltage stability and FACT devices is not explored in this research, and none of the nonlinearities are considered in [(3)], [(15)]. AVR is employed in both areas of the proposed article, and eigenvalue analysis is performed on each scenario to determine system stability. Robustness is also evaluated under various load circumstances. This article also addresses the effect of a boiler equipped with a reheat turbine. This publication does not include an eigenvalue analysis for the preferred power system (PS) mode, neither is AVR included in the PS for controlling the reactive power [(16)]. This given study measures non-linearity and the influence of the FACT-Device, as well as eigenvalue analysis and robustness testing at various loading situations. In this literature no eigenvalue analysis is performed and nonlinearities are also not integrated into IPS, effect of energy storage and FACT Device is also not included in this presented work and Effect of AVR is also not included in [8]. In this present work all these points are incorporated to improve the usefulness of the PS.

The Proposed study for LFC makes the following key contributions: (i) Configuration of a multi-area, multi-source interconnected power system (MAMS-IPS) with three generating units in each region including AVR in both areas. (ii) Implementation of a hybrid PI-PD controller with parameters modified by the Artificial Bee Colony (ABC) optimal approach. (iii) Results obtained from the proposed approach were compared to previously publish optimized technique-based controllers such as TLBO-PID, FDA-PID, and SSA-PID. (iv) SMES-UPFC in MAMS-IPS. The parameters of SMES-UPFC are enhanced using the ABC approach. (v) Rigidness of the controller for different loading conditions is verified at different DPMs, as well as for non-linearity such as governor dead band (GDB) and generation rate constraints (GRC). (vi) Eigenvalue analysis is implemented to ensure system stability in various scenarios.

2 System Description

This presented work is based on a restructured energy network (REN) including six power generating units, GENCO-1 and GENCO-4 related to the thermal unit, hydro with GENCO-2 and GENCO-5, and for gas is GENCO-3 and GENCO-6. The two distribution firms are included in this presented power system as DISCO-1 and DISCO-2 in area-1, and DISCO-3 and DISCO-4 in area-2. Energy storage devices SMES have been integrated in every region. Figure 1 displays the Transfer Function Model (TFM) for the IPS. The number of rows and columns in the matrix represents the total number of GENCOs and DISCOs, respectively. DISCOs can purchase power from any GENCO in their area at reasonable rates. The DPM will demonstrate the whole transaction which is given by **equation 1**. Each area gets a load perturbation of 10% (0.01 P.U). The Matlab/Simulink software is used to develop Transfer-Function (TF) models. The data set for the MAMS-IPS Transfer Function Model can be found in Appendix 1. The ABC algorithm is used to optimize the controller settings (PI-PD). The detailed modeling of the Power system illustrated in this present work is given in [1], [2], [7], [8].

$$DPM = \begin{bmatrix} \rightarrow & DISCO_1 & DISCO_2 & DISCO_3 & DISCO_4 \\ GENCO_1 & cpf_{11} & cpf_{12} & cpf_{13} & cpf_{14} \\ GENCO_2 & cpf_{21} & cpf_{22} & cpf_{23} & cpf_{24} \\ GENCO_3 & cpf_{31} & cpf_{32} & cpf_{33} & cpf_{34} \\ GENCO_4 & cpf_{41} & cpf_{42} & cpf_{43} & cpf_{44} \\ GENCO_5 & cpf_{51} & cpf_{52} & cpf_{53} & cpf_{54} \\ GENCO_6 & cpf_{61} & cpf_{62} & cpf_{63} & cpf_{64} \end{bmatrix} \tag{1}$$

Whereas C_{pf} represents contract participation factor, In the DPM, the ij^{th} entry represents the fraction of total load power contracted by the j^{th} DISCO (column) from the i^{th} GENCO (row), the sum of all C_{pf} in a column equals unity. DISCO's in a restricted power system are DISCOM companies responsible for delivering the power supply to consumers. From GENCO's power is purchased and distribute to users. The DISCO's Participation Matrix (DPM) visualizes the contract between GENCO's and Discos.

The Automatic Voltage Regulator (AVR) is an essential component of an electricity grid.

AVR Transfer Function model is illustrated in [2].

2.1 Interlinked Power System Network Nonlinearities

MAMS-IPS includes three nonlinearities: GRC, GDB, and boiler. A critical mechanism knows as GRC is employed For LFC which regulate the synchronous generators response with respect to frequency deviations. The maximum limit is determined as (0.5×10^{-2}) and The minimum limit for the GRC band is set as (-0.5×10^{-2}) and detail modeling of GRC is given in (17). The governor dead band determines the range in which the alternator governor does not respond to a change in frequency deviation. The governor's sensitivity decreases as the dead band widens and increases as the dead band narrows illustrated in [17]. In this proposed model, the GDB maximum value is (0.8), and the smaller limit is (-0.06). All values are per unit. For the LFC system, a drum type boiler is implemented. They provide stable and reliable steam supply for power generation. Application of boiler in LFC model is illustrated in [18].

2.2 SMES and UPFC Modeling For LFC-AVR

It comprises of a superconducting magnetic coil for storing electrical power illustrated in [4], [19]. SMES is utilized in each region to mitigate the frequency response fluctuation. K_{SMES} Is the stabilizing gain and T1, T2, T3, and T4 are the time-constant for

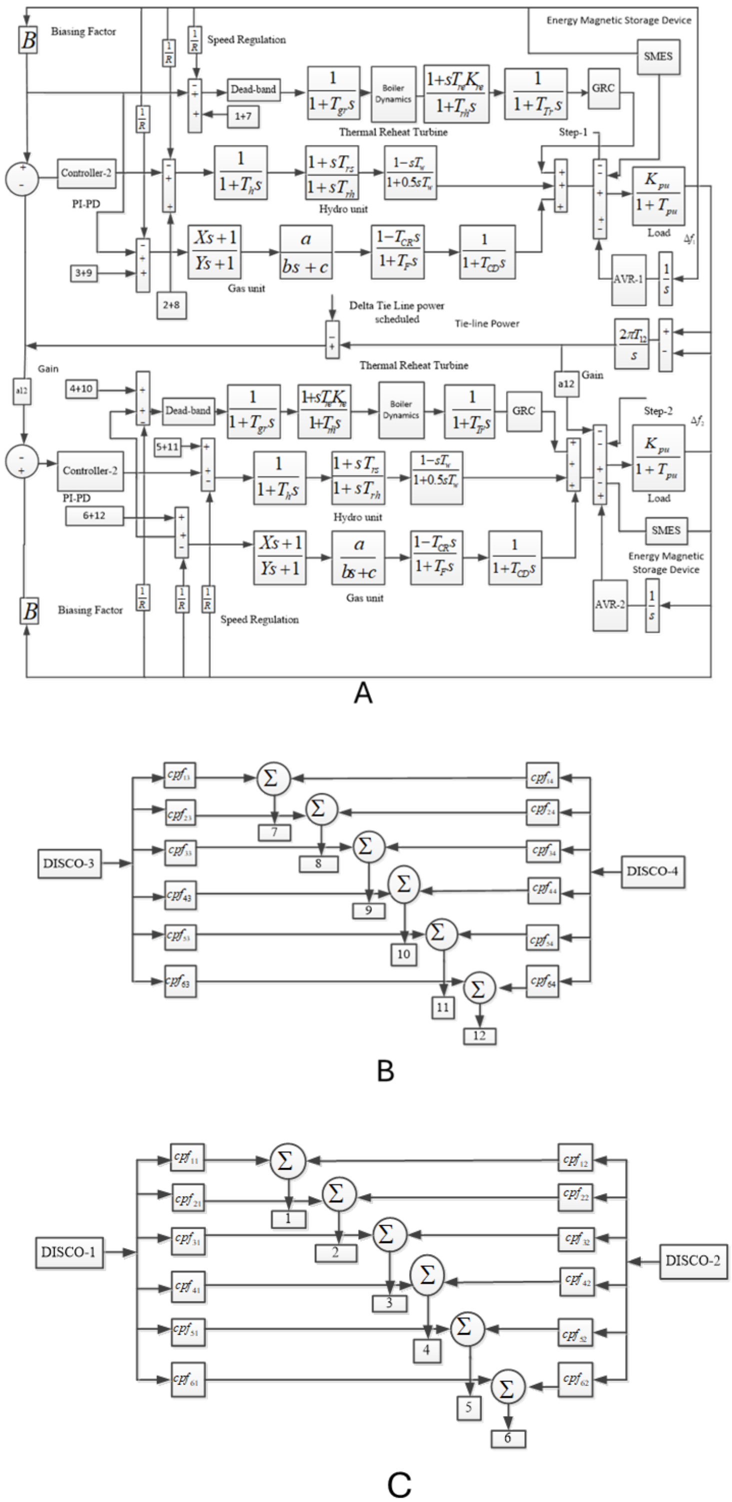

Fig 1. (A) MAMS-IPS for Deregulated environment incorporated with Nonlinearities and SMES (B) and (C) Sharing of Contract Participation Factors and Discos [1], [7], [8]

the lead-lag compensator used by SMES. UPFC can regulate each characteristic, such as impedance, voltage, and phase angle that are responsible for the power flow throughout interconnected transmission lines (TL) illustrated in. UPFC serves three different tasks: reactive power shunt compensation, series compensation, and phase angle variation. Active and reactive power regulation also performed by it. The Detail Description of UPFC is given in [19]. The Expression for UPFC is given below in **equation 2**.

$$\Delta P_{UPFC}(s) = \frac{1}{1+sT_{UPFC}}\Delta F_1(s) \tag{2}$$

Where, $T_{UPFC}$is the Time-constant for UPFC

3 Methodology

3.1 Artificial Bee Colony Algorithm

The ABC algorithm was inspired by honeybees' foraging behavior. Bees communicate with each other to discover the finest food source. Similarly in the ABC algorithm, artificial bees communicate to explore the search space and identify the best answer. A flow chart of the optimization technique and its mathematical equation along with steps to create this optimization algorithm is illustrated in [20]. There are three components. Employed bees exploit food sources and exchange information about their quality with other bees. The second kind is onlooker bees, who select food sources to exploit it based on information supplied by employed bees. When hired bees are unable to discover better solutions, scout bees hunt for alternative Sources of nutrition. Scaling Variable extreme and least values are taken between (0-5). The plant output such as (Δf_i,ΔV_i,$\Delta p_{i,j}$) is used to construct the fitness function, which is then delivered to the ABC algorithm as input along with the approach control parameters. The algorithmic steps of the suggested methodology for ABC technique is available in the pseudo code provided in [?]. The proposed ABC optimized method setting is provided as follows, colony size is 50, L=360, No-looker=50, Npop=50, a=1, No iteration is 100, Variable extreme value is 5, Variable lowest value is -5. Variable size for three cases is (1, 20). Best cost value for case-1 is given as 0.01334 and for case-2 it is 0.087, similarly for case-3 it is 0.002647.

3.2 Proposed Methodology for MAMS-IPS

This article describes a modified PID controller into a PI-PD hybrid controller, which is imposed to lower the frequency and voltage deviations along with Automatic Control Error (ACE) near zero. The ABC-optimized method improves the gain of the proposed controller. The transfer function model of the proposed controller is given below, and the output of the given controller is described in **equation 3**.

$$U(s) = \left(K_{p1} + \frac{K_i}{s}\right)E(s) - (K_{P2} + K_d s)Y(s) \tag{3}$$

U is a control signal and E is Error signals, difference of output (Y(S)) and Reference signal (R(S)) is Correspondingly given by equation 4

$$E(s) = Y(s) - R(s) \tag{4}$$

By Optimization the costs Function (J), the PI-PD controller gains are tuned. The ABC refinement methodology is recommended for obtaining best gains of the suggested controller. To optimize the gain and minimizing the (ACE) error signal, several performance indices are taken together into consideration. Mainly there are ISE, ITAE, IAE and ITSE objective indices taken in LFC study.

$$X_{ISE} = \int_0^t \left(\Delta f_i^2 + \Delta f_j^2 + \Delta v_{ii}^2 + \Delta v_{ij}^2 + \Delta P_{tieij}^2\right).dt \tag{5}$$

For obtaining the tuned parameters by implementing ABC optimization technique, objective function from equation 5 is proposed. The optimized parameters of PI-PD controller for both areas of LFC-AVR MAMS-IPS for different cases are demonstrated in Table 1. Parameters for UPFC Followed by SMES are given in below Table 2. In the presented work, the range of optimum parameters is defined by coder, the range of the suggested controller is regarded between (-2 to 2). The optimized Tuned parameters of UPFC and SMES are obtained using ABC technique. Responses obtained with the help of optimized UPFC-SMES are improved it is illustrated in Figure 9. SMES range is define between $K1_{1\max 1\min}$, $Tsmes_{smes\max smesmin}$. Similarly, by implementing the suggested approach the optimal settings for the UPFC is taken as $\mathrm{K\_upfc}_{\mathrm{min}_{\le \mathrm{K\_upfc} \le \mathrm{K\_upfc}}\mathrm{max}}$, $\mathrm{T\_upfc}_{\mathrm{min}_{\le \mathrm{T\_upfc} \le \mathrm{T\_upfc}}\mathrm{max}}$.

Table 1. Variable of the suggested PI-PD controller for different cases (MAMS-IPS)

Suggested-PI-PD controller parameters For Case-1					
S. no	**Proposed controller PI-PD**	Δf_1	Δf_2	ΔV_1	ΔV_2
1	K_{p1}	0.2061	0.9900	0.0811	1.0831
2	K_I	0.0524	0.1121	0.2718	0.02301
3	K_{p2}	2.2370	0.1465	0.0407	0.0201
4	K_d	0.0369	0.0852	0.04991	0.0224
Suggested-PI-PD controller parameters For Case-2					
S. no	**Proposed controller PI-PD**	Δf_1	Δf_2	ΔV_1	ΔV_2
1	K_{p1}	0.0135	0.2149	0.0450	0.0184
2	K_I	0.01001	0.0249	0.01891	0.0219
3	K_{p2}	2.86253	0.2390	0.2327	0.0154
4	K_d	0.9186	0.2149	0.02251	0.8388
Suggested-PI-PD controller parameters For Case-3					
S. no	**Proposed controller PI-PD**	Δf_1	Δf_2	ΔV_1	ΔV_2
1	K_{p1}	0.07630	0.1010	0.01447	0.71628
2	K_I	0.0628	0.0258	0.4493	0.3178
3	K_{p2}	1.3241	1.6260	1.2484	1.8942
4	K_d	0.8915	0.6561	0.2370	0.4069

Table 2. Tuned parameters for SMES and UPFC incorporated for MAMS-IPS

S. No		**Case-1**	**Case-2**	**Case-3**	**UPFC**	T_{UPFC}
1	**SMES**	Δf_1**and**Δf_2	Δf_1**and**Δf_2	Δf_1**and**Δf_2		
2	K1	0.0618	0.7162	1.3375	Cases-1	0.05601
3	K2	0.0100	1.8260	1.1272	Cases-2	0.0249
4	K3	1.3255	0.0436	0.4493	Cases-3	0.0337
5	K4	0.0229	0.0628	0.0166		
6	K_{SMES}	0.0201	0.8915	0.2561		
7	T_{SMES}	1.4001	0.0591	1.3484		

4 Result and Discussion

The two-area IPS in a deregulated environment is analyzed and the simulation results are presented in this section. A comprehensive simulation analysis was conducted with PI-PD controllers, and the incorporation of SMES-UPFC was investigated as a means of enhancing the system's LFC mechanism. Various contract arrangements in the deregulated electricity network have been the subject of case studies. The simulations taken into account all GENCOs' role in frequency regulation, including their ($apfs$) and DPM. GENCOs' responses have been verified using calculated values for reliable results. This study determines how well the suggested control method optimized using the ABC algorithm works in a market for deregulated electricity. Figure 10 shows the iteration curves produced for all three situations. Sensitivity analysis examines the impact of nonlinearities such as GRC, GDB, and Boiler on the proposed controller's effectiveness under realistic settings. Three situations are demonstrated for testing the power system responses:

4.1 (Case-1) Poolco-based transaction (PBT)

Here, as stated in the DPM, DISCOs are limited to obtaining power from GENCOs inside the boundaries of their contracted zone. Only area-1 is subject to a 0.01 P.U. load fluctuation. The power requirements in this region are predicted by the DISCO-1 and DISCO-2 to be 0.005 P.U. in MW, or ΔP_{L1} and ΔP_{L2} respectively. Because DISCO-3 and DISCO-4 have zero load demands (ΔP_{L3} and ΔP_{L4} = 0 P.U. MW), Area-2's power demand variation is zero, and the predicted DPM is also zero. In

PBT, the set of DPM given by **equation 6**, determines how power is divided across DISCOs and current GENCOs.

$$DPM = \begin{bmatrix} 0.3333 & 0.3333 & 0 & 0 \\ 0.3333 & 0.3333 & 0 & 0 \\ 0.3333 & 0.3333 & 0 & 0 \\ 0 & 0 & 0 & 0 \\ 0 & 0 & 0 & 0 \\ 0 & 0 & 0 & 0 \end{bmatrix} \tag{6}$$

In a steady-state for PBT, the power generation of GENCOs can be estimated using the following method: $\Delta P_{GENCO-1} = 0.333 \times 0.005 + 0.333 \times 0.005 + 0 \times 0 + 0 \times 0 = 0.00333$ P.U MW, $\Delta P_{GENCO-2} = 0.0033$,$\Delta P_{GENCO-3} = 0.0033$, DISCOs 3 and 4 weren't looking for power in area 2, hence GENCO's outputs in that area are nothing. $\Delta P_{GENCO-4} = \Delta P_{GENCO-5} = \Delta P_{GENCO-6} = 0$.

A step load perturbation is delivered to each zone of MAMS-IPS. The variation in Frequency and tie-line power flow is demonstrated in Figure 2 for case-1 for both the interconnected area. Figure 3 shows the voltage deviation of both areas illustrated for case-1. By observing the figures it is concluded that the steady state error (SSE) of the responses is reduced near to zero. By implementing the suggested hybrid PI-PD optimized through ABC algorithm controller, the values of performance indices for case-1 obtained is provided in Table 3. The settling time (ST) is $\Delta f_{ST}^{area-1} = 8.1966\,\text{sec}$ and for area-2 it is $\Delta f_{ST}^{area-2} = 9.4818\,\text{sec}$ similarly for $\Delta P_{ST}^{area-1,2} = 10.0301\,\text{sec}$. Value of objective function for case-1 is ISE=0.0008747, IAE=0.007977, ITAE=0.009226 and ITSE=0.0030216. By analyzing the Figure 4 it is clear that the electricity production by the Gencos is equal to the power demanded by the load and by Discos of both areas. Similarly, response of participation power output generated by Gencos of area-2 is obtained.

Table 3. Compares every scenario based on performance indices based on Proposed ABC-PI-PD

S.no	Different cases	ITAE	ITSE	IAE	ISE
1	Case-1	0.009	0.0030	0.007	0.0008
2	Case-2	0.006	0.0091	0.009	0.0001
3	Case-3	0.009	0.0012	0.002	0.0005

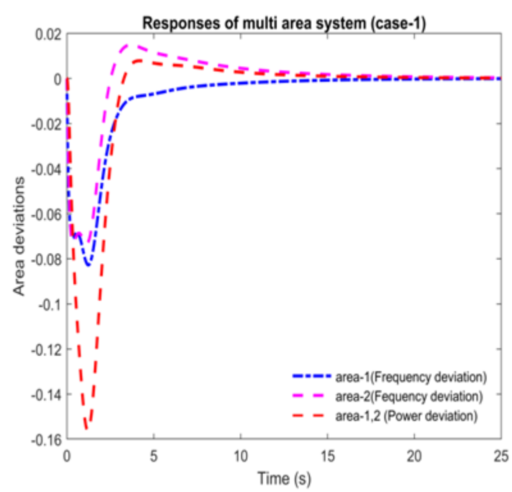

Fig 2. Different Responses obtained for MAMS-IPS for case-1 (PBT Scenario)

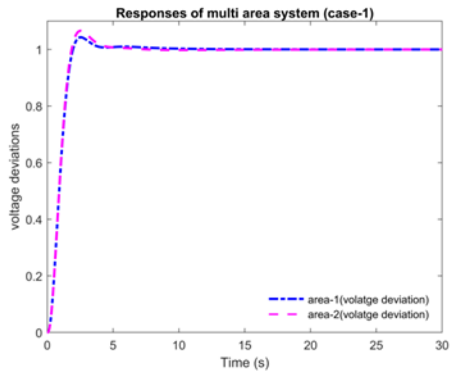

Fig 3. Voltage response obtained for MAMS-IPS for case-1 (PBT Scenario)

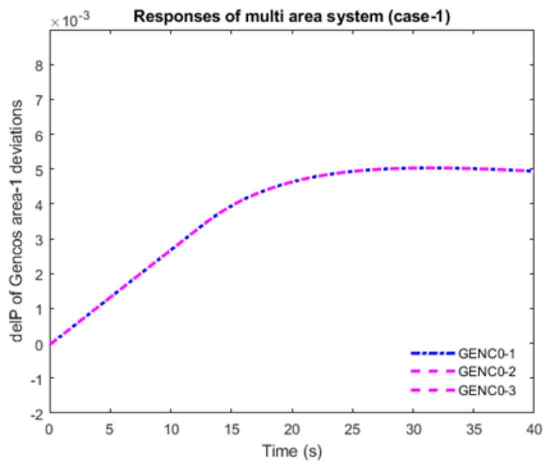

Fig 4. Power response of Gencos for area-1 in P.U MW for MAMS-IPS

4.2 (Case-2) Bilateral based transaction (BBT)

Bilateral transactions between a GENCO and a DISCO can take place in any industry, as long as both sides agree to the contract conditions. DISCOs deal with GENCOs based on the following DPM is given by **equation 7**.

$$DPM = \begin{bmatrix} 0.2 & 0.1 & 0.3 & 0 \\ 0.2 & 0.2 & 0.1 & 0.166 \\ 0.1 & 0.3 & 0.1 & 0.166 \\ 0.2 & 0.1 & 0.1 & 0.333 \\ 0.2 & 0.2 & 0.2 & 0.166 \\ 0.1 & 0.1 & 0.2 & 0.166 \end{bmatrix} \tag{7}$$

The $cpfs$ states that DISCOs are able to demand 0.005 p.u. MW of energy from GENCOs within their governing area, according to regulations with the BBT in the DPM. Thus, 0.01 p.u. MW indicates the total load disturbance in each area. After a step load perturbation, the power outputs of all GENCOs are divided into areas 1 and 2, as shown below: $\Delta P_{GENCO-1} = 0.2 \times 0.005 + 0.1 \times 0.005 + 0.3 \times 0.005 + 0 \times 0.005 = 0.0030$ P.U MW $\Delta P_{GENCO-2} = 0.00333$, $\Delta P_{GENCO-3} = 0.0033$, $\Delta P_{GENCO-4} = 0.00368 \Delta P_{GENCO-5} = 0.003833 \Delta P_{GENCO-6} = 0.00283$. The variation in Frequency and tie-line power flow is demonstrated in Figure 5 for case-2. The values of performance indices for case-2 are provided in Table 3. The settling time (ST) for frequency departure of area-1 is $\Delta f_{ST}^{area-1} = 8.3582\,\text{sec}$ and for area-2 it is $\Delta f_{ST}^{area-2} = 9.9782\,\text{sec}$ similarly for $\Delta P_{ST}^{area-1,2} = 9.0301\,\text{sec}$. Value of objective function for case-2 is ISE=0.0001152, IAE=0.006088, ITAE=0.00918 and ITSE=0.00907.

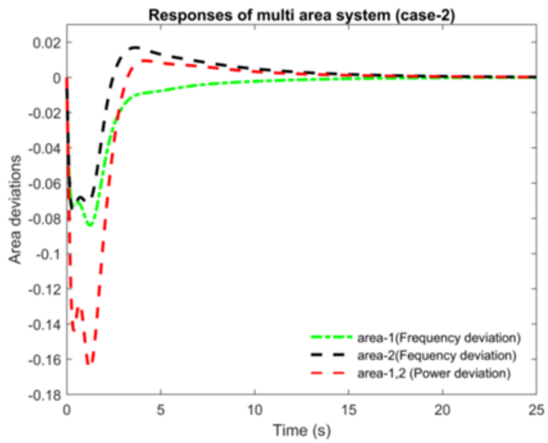

Fig 5. Different Responses obtained for MAMS-IPS for case-2 (BBT Scenario)

4.3 (Case-3) Contract violations

DISCOs may, in rare occasions, demand excessive electricity in violation of a contract. Within the same control territory as the DISCO, GENCOs are required to supply un-contracted electricity. In the control area, this type of demand is displayed as a local load. Take instance 1 and modify it as follows: A further 0.01 MW of electricity is needed for DISCO-1. The entire local load in region of control 1 is ascertained as

$\Delta P_{D1} =$ (Load of DISCO-1) + (Load of DISCO-2)$(0.05+0.01)+(0.05) = 0.11$ P.U MW

Similarly, the total regional load for control area-2 becomes as

$\Delta P_{D1} =$ (Load of DISCO-3) + (Load of DISCO-2)$(0)+(0) = 0$ P.U MW

The variation in Frequency and tie-line power flow is demonstrated in Figure 6 for case-3. The settling time (ST) for frequency deviation of area-1 is $\Delta f_{ST}^{area-1} = 8.0919\,\text{sec}$ and for area-2 it is $\Delta f_{ST}^{area-2} = 7.4637\,\text{sec}$ similarly for $\Delta P_{ST}^{area-1,2} = 9.2327\,\text{sec}$. Value of objective function for case-3 is ISE=0.0005851, IAE=0.002674, ITAE=0.0097 and ITSE=0.001209.

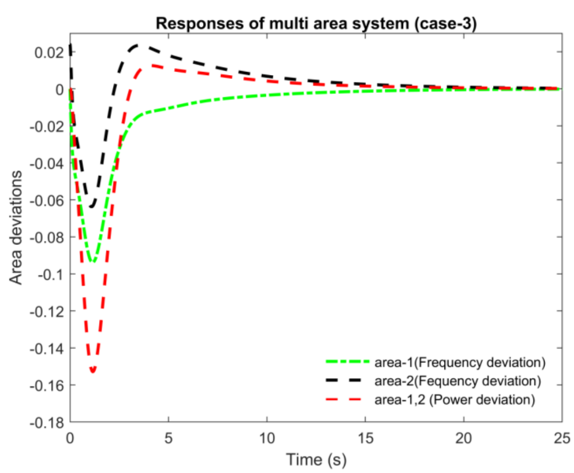

Fig 6. Different Responses obtained for MAMS-IPS for case-3 (CVBT Scenario)

4.4 Sensitive Analysis

For analysis the usefulness of the proposed controller it is implemented for all the three cases considered in this article for LFC study in deregulated environment. For the Rigidness testing of hybrid PI-PD controller Case-2 is being evaluated for MAMS-IPS. Responses obtained for frequency and Tie-line power are associated with recently published literature controllers. Proposed controller shows more promising results when compared with the result of controller published in literature such as TLBO-PID, SSA-PID and FDA-PID. The outcomes of the suggested controller are compared on the basis of Settling Time (ST) and peak time (PT). By the suggested controller the settling time (ST) of the frequency response of area-1 and area-2 settled at 5.24 sec and 8.68 sec which are quite better as compared to the recently published controller. Settling Time of $\Delta P_{1,2}$ response is 11.53 sec. Comparison of frequency response is illustrated in Figure 7. Table 4 shows the comparison on the basis of Settling Time (ST) and Table 5 shows comparison on the basis of peak Time (PT). The improvement in the (ST) for Δf_1 and Δf_2 responses is 39.1% and 45.06 %. Similarly, the improvement in the $\Delta P_{1,2}$ response (ST) is 22.31% when the suggested controller result is compared with the literature bases TLBO-PID controller.

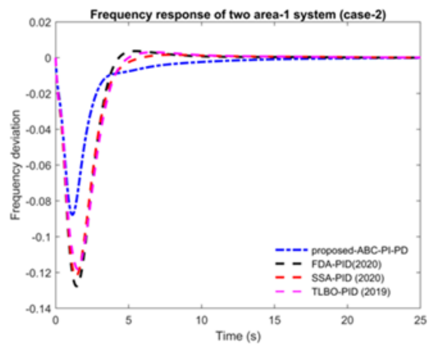

Fig 7. Frequency response of area-1 for case-2 (BBT Scenario) and compared with recently published controller (1, 7, 8)

Table 4. Comparison of the proposed (PI-PD-ABC) controller exhibited for LFC-AVR-SMES-UPFC (case-02) based on Settling Time (ST) from the latest published research

S. No	Parameters of system	Suggested ABC (PI-PD) controller (sec)	SSA-PID (8) (sec)	FDA-PID (1) (sec)	TLBO-PID (7) (sec)
1	ΔF_1	5.2456	7.0208	7.0014	8.2055
2	ΔF_2	8.6810	10.3	11.05	12.2
3	ΔP_{12}	11.58	15.7	14.9	13.6

Table 5. Comparison of the proposed (PI-PD-ABC) controller exhibited for LFC-AVR- SMES-UPFC (case-02) based on peak Time (PT) from the latest published research

S. No	Parameters of system	Suggested ABC (PI-PD) controller (sec)	SSA-PID (8) (sec)	FDA-PID (1) (sec)	TLBO-PID (7) (sec)
1	ΔF_1	0.000231	0.00541	0.0011	0.0032
2	ΔF_2	0.00004019	0.0004046	0.000276	0.00072
3	ΔP_{12}	0.00017345	0.0004706	0.000295	0.000356

The step load is increased by 10% as by absorbing the outcomes of MAMS-IPS it is concluded that by varying the load, The error during steady-state conditions remains close to zero. So by this the rigidness of the suggested controller is verified. The Δf responses at various loading condition is provided in Figure 8. The effectiveness of the energy storage device (SMES) following with Fact device (UPFC) for the LFC is illustrated in Figure 9.

By the SMES-UPFC the percentage improvement of settling time (ST) is 49.9% for area-1 and 60.1% for area-2 and tie-line power (ST) is improved by 38.03% when compared with the responses of MAMS-IPS without SMES-UPFC. The iteration graph for the different three cases is illustrated in Figure 10. For commenting on the Sustainability of the projected MAMS-IPS eigenvalue analysis is carried out. It is analyzed that all the eigenvalues for all three different cases lie at the left-hand side of the S plane, this analysis justified that the power systems (MAMS-IPS) taken in this Study are Stable. The eigenvalues for all three cases are demonstrated in Table 6.

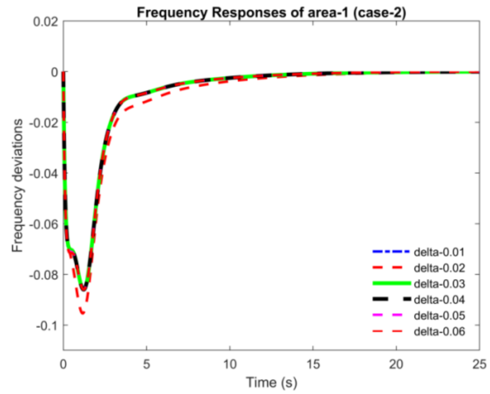

Fig 8. Frequency response of area-1 for case-2 (BBT scenario) at different loading condition

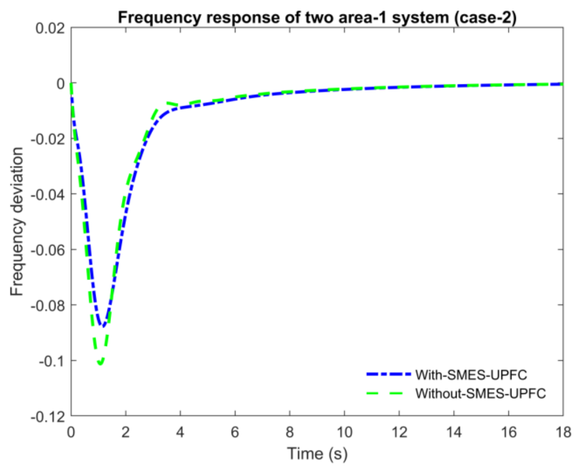

Fig 9. Frequency response for area-1 with SMES-UPFC and without for case-2 (BBT scenario)

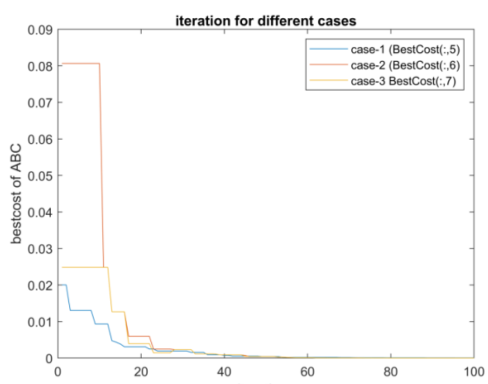

Fig 10. ABC Convergence Characteristics for the different cases

Table 6. Eigenvalues for various cases determined using the ABC-PI-PD optimization approach

S. NO	CASE-1	CASE-2	CASE-3
1	-3.3333 + 0.0000i	-3.3333 + 0.000i	-3.3333 + 0.000i
2	-0.10000 + 0.0000i	-0.1000 + 0.000i	-0.1000 + 0.000i
3	-3.3333 + 0.0000i	-3.333 + 0.000i	-3.3333 + 0.000i
4	-0.1000 + 0.0000i	-0.100 + 0.000i	-0.1000 + 0.000i
5	-9.7710 + 0.000i	-0.0383 + 0.000i	-9.9844 + 0.000i
6	-1.0236 + 0.0000i	-0.0526 + 0.000i	-1.1697 + 0.000i
7	-4.84518 + 0.0012i	-1.841 + 0.0061i	-9.7334 + 0.000i
8	-9.8451 + 0.0028i	-1.848 - 0.0062i	-9.619 + 0.0000i
9	-5.3400 + 0.0000i	-1.5118 + 0.000i	-8.382 + 0.0000i
10	-5.1784 + 0.0000i	-1.523 + 0.0000i	-7.877 + 0.0000i
11	-4.1753 + 0.0000i	-11.702 + 0.000i	-2.056 + 0.0000i
12	-3.4028 + 0.0000i	-11.669 + 0.000i	-2.321 + 0.0000i
13	-7.0280 + 0.0000i	-12.500 + 0.000i	-1.833 + 0.0178i
14	-0.60459 + 0.000i	-12.500 + 0.000i	-1.845 + 0.01787i
15	-1.9595 + 0.0000i	-7.089 + 0.1821i	-2.283 + 1.3261i
16	-1.8144 + 0.0000i	-7.081 + 0.1822i	-2.2919 +0.3261i
17	-19.8143 + 0.000i	-0.3120 + 4.385i	-10.323 + 0.000i
18	-3.1784 + 5.803i	-0.3120 + 4.385i	-12.500 + 0.000i
19	-3.1884 - 5.803i	-0.1677 + 3.638i	-12.100 + 0.000i
20	-10.773 + 0.0000i	-0.1677 + 3.6389i	-7.2460 + 0.000i
21	-10.7710 + 0.000i	-0.3511 + 2.4821i	-6.8815 + 0.000i
22	-6.5058 + 2.930i	-0.3517 + 2.4821i	-0.3448 + 4.404i
23	-6.5051 + 2.9307i	-0.5011 + 2.4991i	-0.3418 + 4.4214i
24	-12.500 + 0.000i	-0.5019 + 2.499i	-0.0829 + 3.5464i
25	-12.500 + 0.000i	-3.1699 + 0.000i	-0.0819 + 3.54164i
26	-4.623 + 0.0000i	-3.1835 + 0.000i	-0.9882 + 2.547i
27	-3.7806 + 0.000i	-2.4130 + 0.000i	-0.9882 + 2.5439i
28	-1.1771 + 1.43i	-2.0778 + 0.000i	-3.2079 + 0.000i
29	-1.1779 + 1.434i	-0.2447 + 0.7490i	-3.1501 + 0.000i
30	-1.210 + 1.4044i	-0.2447 + 0.74670i	-2.4904 + 0.000i
31	-1.2104 + 1.4044i	-1.1261 + 0.0000i	-2.017 + 0.0000i
32	-2.2977 + 0.000i	-0.8829 + 0.0363i	-0.223 + 0.81266i
33	-1.8715 + 0.000i	-0.8801 + 0.03631i	-0.227 + 0.81266i
34	-1.1103 + 0.203i	-1.4461 + 0.0000i	-0.8628 + 0.000i
35	-1.1103 + 0.2031i	-1.4469 + 0.0000i	-0.4971 + 0.3309i
36	-0.6395 + 0.3416i	-0.0611 + 0.0000i	-0.499 + 0.331519i
37	-0.639 + 0.34165i	-0.0351 + 0.0000i	-0.468 + 0.0000i
38	-0.6131 + 0.2858i	-0.09921 + 0.0000i	-1.4469 + 5.871e-16i
39	-0.61302 + 0.2858i	-0.0992 + 0.0000i	-1.4167 + 5.87221e-16i
40	-0.8791 + 0.03131i	-0.00352 + 0.0113i	-0.060123 + 0.000i

5 Conclusion

This study uses a multi-area, multi-source power system within a deregulated scenario for the Load Frequency Control (LFC) analysis. The Artificial Bee Colony (ABC) algorithm is utilized to optimize the PI-PD controller parameters. Secondary units, such as the unified power flow controller (UPFC) and superconducting magnetic energy storage (SMES), are added to the primary unit. These units, which are integrated into contemporary power systems (PS), offer a comprehensive and progressive solution to address the challenges associated with PS. The frequency response obtained by the suggested controller settled at 5.24 sec and 8.68 sec. Which are quite impressive as related to the recently published controller outputs, the settling time of the Tie-line power response is 11.53 sec. The enhancements in the (ST) for frequency responses of both areas are 39.1% and 45.06 %. Similarly, power response improvement is 22.31%. The stiffness of this hybrid PI-PD controller is verified under a range of operating situations, and in a deregulated environment, this optimized controller guarantees reliable and efficient frequency regulation. To improve field excitation and manage reactive power in the producing unit, the study is further expanded by including an automated voltage regulator (AVR) in both domains. It appears that the corresponding estimated (desired) values match the actual numbers of generators and tie-line power exchanges of GENCOs produced by the power system's MATLAB simulation model. By incorporating SMES-UPFC in both areas of MAMS-IPS the improvement of settling time (ST) is 49.9% and 60.1% and Tie-line power (ST) is improved by 38.03% when compared with MAMS-IPS responses without SMES-UPFC. Furthermore, eigenvalue analysis is carried out for each scenario. The investigation may be expanded by taking into account various energy storage technologies that can be integrated with PS and their impacts taken into account, as well as various renewable energy sources like solar and wind. For even more efficacy, a hybrid controller can be used in place of a fractional PID controller.

6 Appendix 1

freq = 50 Hz; (*Biasing − factor*) "*B*" = 0.45 MW/Hz; $P_R = 2000_{MW(rating)}$, *Load*"P_L" = $1740_{MW(small-loading)}$; (*Regulation*)"*R*" = $2.4_{Hz/p.uM}$ (*participationfactor*) "$pf_{ii} = pf_{ji}$" = 0.49666; (*participationfactor*) "$pf_{ij} = pf_{jj}$" = 0.37814; (*participationfactor*) "$pf_{ij} = pf_{jj}$" = 0.1522; T_{pu} = 11.49; K_{pu} = 68.9566 Hz/p.u; (*Tie − Line*)"T_{12}" = 0.0433; *gain*"a_{12}" = − 1. Thermal: (*governor − Time*)"T_{gr}" = 0.08 sec; (*Reheat − Turbine*) "T_{re}" = 10 sec; (*reheat − gain*) "K_r" = 0.30, (*Turbine − Time*)"T_{tr}" = 0.3 sec. Hydro:- (*hydro − Time*) "T_h" = 28.75, (*hydro − Turbine*) "T_{rs}" = 5 sec; (*Turbine*) "T_{rh}" = 0.2 sec; (*Time − constant*) "T_T" = 1 sec. 0.5 sec; (*combuction − time*)"*c*" = 1 sec; Gas:-(*gas − turbine*)"*b*" = (*Lead − Time*)"*X*" = 0.6 sec; (*Lag − Time*)"*Y*" = 1 sec; (*gas − turbine − combuction*) "T_{cr}" = 0.03 sec; $T_{f1} = T_{f2} = T_f$ = 0.23 sec (*discharge − time*) "T_{cd}" = 0.2 sec, *AVR-Parameters*:- (*amplifier − gain*) "K_A" = 10, (*amplifier − time*) "T_A" = 0.1 sec, (*Exciter − gain*) "K_E" = 1, (*Exciter − time*)"T_A" = 0.4 sec, (*generator − gain*) "K_G" = 0.8, (*generator − time*) "T_G" = 1.4, (*sensor − gain*) "K_s" = 1, (*sensor − time*) "T_s" = 0.05 sec, (*gain*) "P_s" = 1.5, (*AVR − gain*) "K_1" = 0.2, (*AVR − gain*)"K_2" = −0.2 , (*gain*) "K_3" = 0.5,(*gain*) "K_4" = 1.4

References

1) Daraz A, Malik SA, Mokhlis H. Improved-Fitness Dependent Optimizer Based FOI-PD Controller for Automatic Generation Control of Multi-Source Interconnected Power System in Deregulated Environment. *IEEE Access*. 2020;8:197757–197775. https://doi.org/10.1109/ACCESS.2020.3033983.
2) Kalyan CNS, Goud BS, Reddy CR. Comparative Performance Assessment of Different Energy Storage Devices in Combined LFC and AVR Analysis of Multi-Area Power System. *Energies*. 2022;15(2):629. https://doi.org/10.3390/en15020629.
3) Kumar A, Gupta DK, Ghatak SR. A Novel Improved GSA-BPSO Driven PID Controller for Load Frequency Control of Multi-Source Deregulated Power System. *Mathematics*. 2022;10(18):3255. https://doi.org/10.3390/math10183255.
4) Mishra DK, Złotecka D, Li L. Significance of SMES Devices for Power System Frequency Regulation Scheme considering Distributed Energy Resources in a Deregulated Environment. *Energies*. 2022;15(5):1766. https://doi.org/10.3390/en15051766.
5) Nayak PC, Prusty RC, Panda S. Grasshopper optimization algorithm optimized multistage controller for automatic generation control of a power system with FACTS devices. *Protection and Control of Modern Power Systems*. 2021;8(6). https://doi.org/10.1186/s41601-021-00187-x.
6) Gupta DK, Dei G, Soni AK, Jha AV, Appasani B, Bizon N. Fractional order PID controller for load frequency control in a deregulated hybrid power system using Aquila Optimization. *Results in Engineering*. 2024;23:102442. https://doi.org/10.1016/j.rineng.2024.102442.
7) Khamari D, Sahu RK, Gorripotu TS, Panda S. Automatic generation control of power system in deregulated environment using hybrid TLBO and pattern search technique. *Ain Shams Engineering Journal*. 2020;11(3):553–573. https://doi.org/10.1016/j.asej.2019.10.012.
8) Sharma M, Dhundhara S, Arya Y, Prakash S. Frequency stabilization in deregulated energy system using coordinated operation of fuzzy controller and redox flow battery. *International Journal of Energy Research*. 2020;44(4):457–475. https://doi.org/10.1002/er.6328.
9) Biswas S, Roy PK, Chatterjee K. FACTS-based 3DOF-PID Controller for LFC of Renewable Power System Under Deregulation Using GOA. *IETE Journal of Research*. 2021;p. 1–15. https://doi.org/10.1080/03772063.2020.1870874.
10) Morsali J. Fractional order control strategy for superconducting magnetic energy storage to take part effectually in automatic generation control issue of a realistic restructured power system. *Journal of Energy Storage*. 2022;55:105764. https://doi.org/10.1016/j.est.2022.105764.
11) Singh B, Slowik A, Bishnoi SK. Review on Soft Computing-Based Controllers for Frequency Regulation of Diverse Traditional, Hybrid, and Future Power Systems. *Energies*. 2023;16(4):1917. https://doi.org/10.3390/en16041917.

12) Kumar R, Sharma VK. Whale Optimization Controller for Load Frequency Control of a Two-Area Multi-source Deregulated Power System. *International Journal of Fuzzy Systems*. 2019;p. 1–19. https://doi.org/10.1007/s40815-019-00761-4.
13) Jena T, Debnath MK, Sanyal SK. Optimal fuzzy-PID controller with derivative filter for load frequency control including UPFC and SMES. *International Journal of Electrical and Computer Engineering (IJECE)*. 2019;9(4):2813–2821. https://doi.org/10.11591/ijece.v9i4.pp2813-2821.
14) Gorle PK, Naik RS, Prasad CD. Application of the PI-PD cascade control scheme in AGC of a deregulated power system with PV in the presence of communication delay. *International Journal of Ambient Energy*. 2021;43(1). https://doi.org/10.1080/01430750.2021.1997807.
15) Farooq Z, Rahman A, Hussain SMS, Ustun TS. Power Generation Control of Renewable Energy Based Hybrid Deregulated Power System. *Energies*. 2022;15(2):517. https://doi.org/10.3390/en15020517.
16) Shafei MAR, Alzaher ANA, Ibrahim DK. Enhancing load frequency control of multi-area multi-sources power system with renewable units and including nonlinearities. *Indonesian Journal of Electrical Engineering and Computer Science*. 2020;19(2):108–118. https://doi.org/10.11591/ijeecs.v19.i1.pp108-118.
17) Karnavas YL, Nivolianiti E. Harris hawks optimization algorithm for load frequency control of isolated multi-source power generating systems. *International Journal of Emerging Electric Power Systems*. 2023;25(4):555–571. https://doi.org/10.1515/ijeeps-2023-0035.
18) Kalyan CNS. UPFC and SMES based Coordinated Control Strategy for Simultaneous Frequency and Voltage Stability of an Interconnected Power System. In: 1st International Conference on Power Electronics and Energy (ICPEE). 2021;p. 1–6. https://doi.org/10.1109/ICPEE50452.2021.9358576.
19) Kumar NKK, Gopi RS, Kuppusamy R. Fuzzy Logic-Based Load Frequency Control in an Island Hybrid Power System Model Using Artificial Bee Colony Optimization. *Energies*. 2022;15(6):2199. https://doi.org/10.3390/en15062199.
20) Fathy A, Kassem A, Zaki ZA. A Robust Artificial Bee Colony-Based Load Frequency Control for Hydro-Thermal Interconnected Power System. *Sustainability*. 2022;14(20):13569. https://doi.org/10.3390/su142013569.